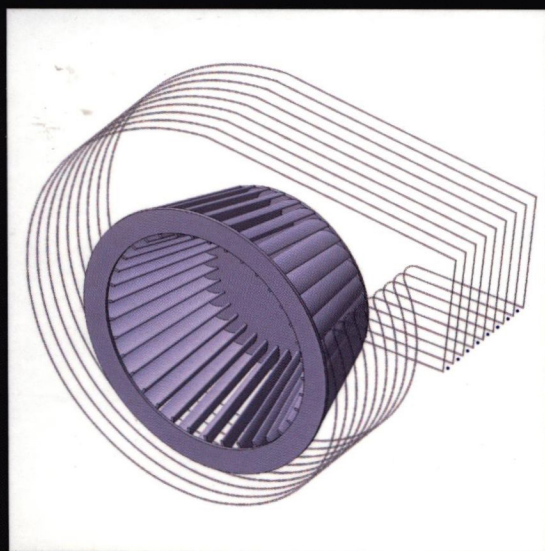


WOODHEAD PUBLISHING
IN MECHANICAL ENGINEERING

Developments in Turbomachinery Flow

Forward curved centrifugal fans

Nader Montazerin, Ghasem Akbari
and Mostafa Mahmoodi



Woodhead Publishing in Mechanical Engineering

Developments in Turbomachinery Flow

Forward Curved Centrifugal Fans

Nader Montazerin

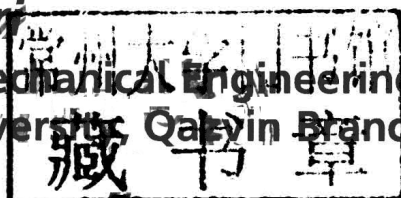
Department of Mechanical Engineering
Amirkabir University of Technology

Ghasem Akbari

Industrial and Mechanical Engineering Faculty
Islamic Azad University, Qazvin Branch

Mostafa Mahmoodi

Department of Mechanical Engineering
Amirkabir University of Technology



AMSTERDAM • BOSTON • CAMBRIDGE • HEIDELBERG
LONDON • NEW YORK • OXFORD • PARIS • SAN DIEGO
SAN FRANCISCO • SINGAPORE • SYDNEY • TOKYO
Woodhead Publishing is an imprint of Elsevier



Woodhead Publishing is an imprint of Elsevier
80 High Street, Sawston, Cambridge, CB22 3HJ, UK
225 Wyman Street, Waltham, MA 02451, USA
Langford Lane, Kidlington, OX5 1GB, UK

Copyright © 2015 Nader Montazerin, Ghasem Akbari and Mostafa Mahmoodu. Published by Elsevier Ltd. All rights reserved.

No part of this publication may be reproduced, stored in a retrieval system or transmitted in any form or by any means electronic, mechanical, photocopying, recording or otherwise without the prior written permission of the publisher.

Permissions may be sought directly from Elsevier's Science & Technology Rights Department in Oxford, UK: phone (+44) (0) 1865 843830; fax (+44) (0) 1865 853333; email: permissions@elsevier.com. Alternatively, you can submit your request online by visiting the Elsevier website at <http://elsevier.com/locate/permissions>, and selecting Obtaining permission to use Elsevier material.

Notice

No responsibility is assumed by the publisher for any injury and/or damage to persons or property as a matter of products liability, negligence or otherwise, or from any use or operation of any methods, products, instructions or ideas contained in the material herein. Because of rapid advances in the medical sciences, in particular, independent verification of diagnoses and drug dosages should be made.

British Library Cataloguing-in-Publication Data

A catalogue record for this book is available from the British Library

Library of Congress Control Number: 2015932043

ISBN 978-1-78242-192-4 (print)

ISBN 978-1-78242-193-1 (online)

For information on all Woodhead Publishing publications
visit our website at <http://store.elsevier.com/>



**Working together
to grow libraries in
developing countries**

www.elsevier.com • www.bookaid.org

Developments in Turbomachinery Flow

Related titles

Schobeiri, *Turbomachinery Flow Physics and Dynamic Performance*, Second edition, Springer, 2012, 9783540223689

Lakshminarayana, *Fluid Dynamics and Heat Transfer of Turbomachinery*, Wiley-Interscience, 1995, 9780471855460

To:

Roshanak, Atekeh, and Zeinab

About the authors

Nader Montazerin is professor of mechanical engineering at Amirkabir University of Technology. He received his BS from Sharif University of Technology, Tehran, Iran (1980) and MS and PhD from Cranfield University of Technology, Bedford, England (1982 and 1985). He immediately started lecturing and research at Amirkabir University of Technology, where his interests are centred on experimental fluid mechanics, turbomachines, compressible flow and applied energy. He has published five books and many journal articles. His industrial activities are on gas turbines, national gas networks and energy efficiency.

Ghasem Akbari is assistant professor of mechanical engineering at Islamic Azad University, Qazvin branch, Industrial and Mechanical Engineering Faculty. He has held this position since 2014. He received his PhD from Amirkabir University of Technology, Tehran, in 2014. He has taught several courses at Islamic Azad University including fluid mechanics, heat transfer, thermodynamics and internal combustion engines. He has served on several provincial/academic projects, including the identification of gas consumption bottlenecks as well as its long-term prediction. He is also interested in experimental and theoretical fluid mechanics and turbulence, particularly in turbomachinery applications. He has published several prominent journal articles on the results of research during his PhD period.

Mostafa Mahmoodi is a PhD candidate in mechanical engineering at Amirkabir University of Technology. He received his BS in mechanical engineering – thermo fluids from Yazd University, Yazd, Iran, in 2007. He received his MS in mechanical engineering – energy conversion from University of Kashan in 2011. His PhD thesis is on numerical and experimental study of aeroacoustic behaviour of squirrel cage fans.

Preface

Squirrel-cage fans are strange. Precious electricity produced by gas and steam turbines is lost to the very inefficient forward-curved fans of the heating and ventilating industry. The research studies on gas and steam turbines are expensive and very competitive worldwide. On the contrary, forward-curved squirrel-cage fans are cheap and simple to build which makes any application of research findings very simple.

The study of the complicated flow field requires advanced measuring techniques such as laser Doppler anemometry. The combination of building different fans, doing performance tests and examination of the flow field with laser anemometry was an attractive research field that was carried out for many years by the team that had written the present book.

Early in this research, modifications to the inlet were proved to be productive. The improvements were far more significant than what was already reported in the literature for other modifications. Later, the present team started with the rotor and the idea of a half-cone rotor and a half-cone with a lean angle that proved to have merit in many cases. Tests on the volute geometry indicated that it was not the shape of the volute cross-section that is important, but the spread angle. Larger spread angle could result in larger flow rates and could override all optimizations to the inlet! Still an optimum spread angle could be defined that gives an aerodynamic flow for a limited space.

It was soon known that optimizations without modelling are very expensive and time-consuming. Simulation of the flow in this fan is not an easy task. Three-dimensional flow, separated flow after the inlet, large number of blades and separated three-dimensional boundary layer inside the blades were all the most important complications in any simulations. Although modelling is not accurate, it was proved to be successful in determining the trends. The modellings were managed to direct research for correct experimental setups and minimum costs.

With the gained experience on fans and laser anemometry, it was natural to move into stereoscopic particle image velocimetry. Squirrel-cage fans are ideal instruments for sample flow measurements in centrifugal turbomachines. They give flat sidewalls and easy access to measuring plane. They rotate slowly and have many features like separations and jet/wake flows that have baffled research studies for a long time.

It was a fortunate occasion that Chandos Publishing invited us to write a book on such fans at this stage. This opportunity provided us with the best chance to review what was achieved during the past twenty-four years. The first four chapters of the book contain our studies on fan performance, fluid flow and fan optimization. Chapter 5 deals with aeroacoustic and sound generation behaviour of the forward-curved

centrifugal fans. Chapter 6 investigates the contribution of jet–wake–volute interactions to flow characteristics and turbulence models which are more advanced, and we expect it to find serious application when the computing capacity for simulating centrifugal turbomachines increases.

We are grateful to acknowledge prior publication of a part of our research in the *Journal of Power and Energy*, *Journal of Turbulence* and *International Journal of Heat and Mass Transfer*. Detailed references are given at the end of each chapter.

I (the first author) have enjoyed the work of two excellent PhD students in the past few years who kindly accepted to be my coauthors in this book. Dr Akbari defended his PhD in 2014 and Mr Mahmoodi shall complete his PhD in a couple of years. There are still many of my old students who contributed to the subject presented in this book and I just name them here with much respect:

Mr Matin Hosseini; Mr Mohammad Reza Shetab Booshehri; Mr Mohammad Reza Najjari; Mr Seyyed Alireza Hosseini; Dr Reza Sepahi Samian; Mr Hossein Akhavan; Mr Soroosh Shahabadi; Mr Masood Nikkhoo; Late Mr Morteza Akbarizadeh; Mr Javad Alinejad; Mr Sina Samarbakhsh; Mr Seyyed Mohammad RezaeiNiya; Mr Arash Heshmat Dehkordi; Mr Saeed Zeinali; Dr Ebrahim Damangir; Mr Mohammad Hassan Hessami Azizi; Mr Mojtaba Gholamian; Mr Mehdi Askari Shahi; Mr Ahmad Kazemi Fard; Mr Ali Toorani; Mr Mohammad Jafar Mahmoodi; Mr Hamid Reza Mirzaei; Dr Seyyed Saeed Mirian; and Dr Ehsan Tooyserkani.

The work is also incomplete if we do not mention other researchers who have done parallel works on squirrel-cage fans round the globe. As far as we know, the only team who has produced continuous research in this field is from Oviedo University in Spain. Their articles have been of much interest and inspiration to us. Other researchers have not been consistent and only produced occasional results. We are indebted to all the inspirations we received from these groups and have tried to cite their works at the end of each relevant chapter.

Nader Montazerin
Tehran
March 2015

Contents

List of figures	ix
List of tables	xv
About the authors	xvii
Preface	xix
1 General introduction of forward-curved squirrel-cage fan	1
1.1 Introduction	1
1.2 Fan geometry	2
1.3 Flow field	4
1.4 Fan performance and noise measurements	6
1.5 Fluid-flow simulation in centrifugal fans	8
1.6 Velocity measurement techniques and their considerations	16
1.7 Final remarks	22
Further reading	22
2 Inlet configuration	25
2.1 Why the inlet is important?	25
2.2 Bell-mouth inlet	25
2.3 Outward inlet	29
2.4 Final remarks	33
Further reading	33
3 Rotor	35
3.1 Half-cone rotors	35
3.2 Lean angle in rotor blades	51
Further reading	57
4 Volute	59
4.1 Volute flow	59
4.2 Slip factor	63
4.3 Volute optimization	68
4.4 Volute width	76
4.5 Double-outlet volute	79
4.6 Final remarks	82
Further reading	82

5	Noise in forward-curved centrifugal fans	85
5.1	Sound parameters	85
5.2	Different types of noise	86
5.3	Modelling of sound generation in fans	87
5.4	Effect of fan components on sound generation	93
5.5	Sound generation of double-outlet squirrel-cage fans	106
5.6	Final remarks	110
	Further Reading	110
6	Contribution of jet–wake–volute interactions to flow characteristics and turbulence models	113
6.1	Role of nonintrusive measurements on examination of complicated turbulent flows	113
6.2	Jet–wake interactions with the volute flow	114
6.3	Geometrical characteristics of tensorial-flow quantities	117
6.4	Challenges in turbulence modelling	122
6.5	Final remarks	129
	References	130
	Index	133

List of figures

Figure 1.1	Geometry of a squirrel-cage fan: (a) three-dimensional geometry of the assembled fan; (b) three-dimensional geometry of the main parts of the fan; (c) two-dimensional views of the fan including the assigned notations in this book.	3
Figure 1.2	Representation of different types of turbomachines on the Cordier diagram.	4
Figure 1.3	Interactive region of flow behind the inlet.	5
Figure 1.4	Characteristics curves of a forward-curved centrifugal fan with cylindrical rotor.	7
Figure 1.5	An experimental setup for noise measurement in centrifugal fan with ducted outlet.	8
Figure 1.6	Comparison of performance of a squirrel-cage fan obtained by experiment and different Reynolds-averaged Navier–Stokes models.	10
Figure 1.7	General configuration of the fan for numerical simulation.	14
Figure 1.8	Sketch of the mesh: (a) on the walls of the considered geometry in numerical simulation; (b) on the rotor blades.	15
Figure 1.9	The measurement volume on the intersection of two laser beams; the fringes are shown by horizontal lines.	18
Figure 1.10	Schematic of a PIV setup that consists of a laser light generator, a laser guide/convertor system, a camera and seeding particles.	18
Figure 2.1	Different squirrel-cage fan inlets: (a) outward inlet; (b) inward inlet; (c) annular inlet.	26
Figure 2.2	Maximum fan flow rate versus nondimensional gap spacing between the rotor and the inlet.	27
Figure 2.3	Geometry of blade tips for a shroud-less rotor.	28
Figure 2.4	Characteristic curves for inward, outward and flat inlets.	29
Figure 2.5	Nondimensional velocity for different normalized flow rates outside the rotor at nondimensional radius 1.09 at (a) 180°; (b) 270°; and (c) 360°. The terms ‘in’ and ‘out’ correspond to inward and outward inlets, respectively.	30
Figure 2.6	Radial and tangential components of the normalized velocity out of the rotor at $\theta = 270^\circ$ for (a) inward inlet and (b) outward inlet.	31
Figure 2.7	Absolute and relative velocity angles out of the rotor of fans with inward and outward inlets at (a) $\theta = 180^\circ$; (b) $\theta = 270^\circ$; and (c) $\theta = 360^\circ$.	32
Figure 3.1	Geometry of different types of rotor: (a) cylindrical rotor ($\alpha = 0$); (b) positive half-cone rotor ($\alpha > 0$); and (c) negative half-cone rotor ($\alpha < 0$). The inlet flow is shown by arrows.	35

Figure 3.2	Comparison of fan performance characteristics for different rotor geometries: (a) pressure coefficient and (b) efficiency.	36
Figure 3.3	General pattern of the flow in the meridional plane of fan. The axial and radial distances are measured relative to the volute backplate and the rotor axis, respectively.	37
Figure 3.4	Static pressure inside (at $r/r_0 = 0.65$) and outside (at $r/r_0 = 1.17$) of the rotor at $\theta = 0^\circ$. Measurements are for different conical angles: (a) $\alpha = +10^\circ$; (b) $\alpha = +5^\circ$; (c) $\alpha = 0^\circ$ (cylindrical rotor); (d) $\alpha = -5^\circ$; and (e) $\alpha = -10^\circ$.	38
Figure 3.5	Location of the centre of vortex for different rotors at angular sections 180° , 270° and 360° .	39
Figure 3.6	Radial normalized velocity out of the cylindrical rotor at $r/r_0 = 1.17$ for different axial locations.	39
Figure 3.7	Axial variation of the radial velocity component for different rotor geometries at (a) $\theta = 25^\circ$ and (b) $\theta = 270^\circ$.	39
Figure 3.8	Axial variation of the tangential velocity component for different rotor geometries at (a) $\theta = 25^\circ$ and (b) $\theta = 270^\circ$.	40
Figure 3.9	Experimental performance characteristics of half-cone rotors with different angles: (a) pressure coefficient versus flow coefficient and (b) efficiency versus flow coefficient.	41
Figure 3.10	Axial variation of radial and circumferential velocity components in $r/r_0 = 1.17$ for three different rotors and two measurement sections: (a) $\theta = 270^\circ$ and (b) $\theta = 360^\circ$.	43
Figure 3.11	Radial velocity component in exit region of a $+10^\circ$ half-cone rotor at various circumferential locations. Measurements are at $r/r_0 = 1.17$ and $z/B = 0.3$.	44
Figure 3.12	Radial component of normalized velocity in conical rotors for operating points D and E at $r/r_0 = 1.0$ and $r/r_0 = 1.17$. (a) Measurement at section $\theta = 270^\circ$; (b) measurement at section $\theta = 360^\circ$; and (c) repetition of curves for $+10^\circ$ half-cone rotor and similarity of radial velocity profile for $r/r_0 = 1.0$ at $\theta = 270^\circ$ and $r/r_0 = 1.17$ at $\theta = 360^\circ$.	46
Figure 3.13	Circumferential component of normalized velocity in the conical rotors at $r/r_0 = 1.0$ and $r/r_0 = 1.17$. Measurements are at sections (a) $\theta = 270^\circ$ and (b) $\theta = 360^\circ$.	47
Figure 3.14	Axial variation of normalized velocity components (radial and circumferential) at $r/r_0 = 1.17$ and $\Phi = 0.55$ for three different rotors. Letters B, C and F in the legend indicate the operating condition points. Measurements are at sections: (a) $\theta = 270^\circ$ and (b) $\theta = 360^\circ$.	48
Figure 3.15	Axial variation of normalized velocity components (radial and circumferential) at two different operating conditions for cylindrical rotor. Measurements are at (a) $\theta = 270^\circ$ and (b) $\theta = 360^\circ$.	50
Figure 3.16	Axial variation of normalized velocity components (radial and circumferential) at two different operating conditions for the -10° half-cone rotor. Measurements are at (a) $\theta = 270^\circ$ and (b) $\theta = 360^\circ$.	50
Figure 3.17	Cylindrical rotors with different blade alignment: (a) a rotor without lean angle; (b) a rotor with positive lean angle; and (c) a rotor with negative lean angle.	51
Figure 3.18	Prediction of change in efficiency with lean angle of blades for cylindrical and half-cone rotors.	52

Figure 3.19	Reference diameter for a cylindrical rotor and its corresponding half-cone rotor.	52
Figure 3.20	Total head coefficient of $+10^\circ$ half-cone rotors with different reference diameters: rotor #1 with the average diameter as the reference diameter and rotor #2 with the diameter at $z/B = 0.3$ as the reference.	53
Figure 3.21	(a) Total head coefficient and (b) efficiency of fans with cylindrical rotor, $+10^\circ$ half-cone rotor without blade lean angle and $+10^\circ$ half-cone rotor with -2° blade lean angle.	53
Figure 3.22	The axial sections in the volute in which the velocity components are measured.	54
Figure 3.23	Axial variation of radial and circumferential velocity components in two fans with $+10^\circ$ half-cone rotors, one without leaned blades and the other with -2° leaned blades. Measurements are at different flow coefficients: (a) $\Phi = 0.52$ and (b) $\Phi = 0.43$.	55
Figure 3.24	(a) Visual representation of the expected vortex behind the fan inlet and (b) variation of axial velocity component with radius along $z/B = 0.7$ for a $+10^\circ$ half-cone rotor with no lean angle and for various flow coefficients.	55
Figure 3.25	Axial velocity profile in two $+10^\circ$ half-cone rotors, one without leaned blades and the other with a -2° lean angle. Measurements are at various flow coefficients: (a) $\Phi = 0.52$; (b) $\Phi = 0.5$; and (c) $\Phi = 0.43$.	56
Figure 4.1	Nondimensional radial velocity scatter at rotor mid-width ($z/B = 0.5$) and four nondimensional radial positions: (a) $r/r_0 = 1.03$; (b) $r/r_0 = 1.09$; (c) $r/r_0 = 1.15$; and (d) $r/r_0 = 1.21$.	60
Figure 4.2	A sample spectrum of the radial velocity for a point close to the rotor exit. The peak at 53 Hz corresponds to blade passing frequency.	61
Figure 4.3	Nondimensional radial velocity profile (a) and its root mean square (b) along the rotor width at different radial stations.	61
Figure 4.4	Power spectral density of the radial velocity at the frequency of 53 Hz in the meridional plane at different radii.	62
Figure 4.5	Normalized radial velocity component for different inlet configurations and various flow rates at three circumferential sections: (a) $\theta = 180^\circ$; (b) $\theta = 270^\circ$; and (c) $\theta = 360^\circ$.	63
Figure 4.6	A definition for slip factor from ideal (broken lines) and real (solid lines) velocity triangles at the rotor outlet. U_{tip} is the rotor peripheral speed, V is the fluid velocity vector and W is the relative velocity vector.	64
Figure 4.7	Axial variation of slip factor for two different fans. Measurements are at maximum flow rate and $\theta = 360^\circ$.	65
Figure 4.8	Variation of slip factor with fan flow rate.	66
Figure 4.9	Axial variation of slip factor for a fan with $\alpha_s = 7^\circ$. Measurements are at maximum efficiency point ($\Phi = 0.632$) and four different circumferential locations.	66
Figure 4.10	Blade-to-blade variation of velocity components (tangential and radial) and slip factor for a fan with $\alpha_s = 7^\circ$. The profiles are shown for four circumferential ranges: (a) $80 \leq \theta \leq 120$; (b) $160 \leq \theta \leq 200$; (c) $250 \leq \theta \leq 290$; (d) $340 \leq \theta \leq 360$ and $0 \leq \theta \leq 20$.	67
Figure 4.11	Volute profiles with three different boundary curves: Profile 1 based on Eqn (4.1) and Profiles 2 and 3 based on Eqn (4.2).	69

Figure 4.12	Effect of volute profile on head of the fan.	69
Figure 4.13	Squirrel-cage fan with conical volute.	70
Figure 4.14	Effect of conical volutes on the head coefficient of the fan.	70
Figure 4.15	The fan performance curves for three volute size according to the classic definitions of head and flow rate coefficients (Eqns (4.3) and (4.4)).	73
Figure 4.16	The fan performance curves for three volute size according to the casing-based normalized coefficients (Eqns (4.6) and (4.7)).	73
Figure 4.17	Fan performance curves for different volute spread angles using classic definition of the flow coefficient: (a) static head coefficient after Roth (1981) and (b) efficiency.	74
Figure 4.18	A comparison between squirrel-cage fan performance curves using casing-based normalized coefficients: (a) static head and (b) efficiency.	74
Figure 4.19	The advantage of the new definition of nondimensional head in determining an optimum for the volute spread angle: (a) rotor-based (classic) head coefficient and (b) casing-based head coefficient.	75
Figure 4.20	Variation of head coefficient (a) and efficiency (b) with radial flow coefficient for different rotor width-to-diameter ratios.	77
Figure 4.21	Fan head coefficient for various rotor width-to-diameter ratios versus (a) radial flow coefficient and (b) axial flow coefficient.	78
Figure 4.22	Peak performance parameters as a function of rotor width-to-diameter ratio: (a) maximum total pressure coefficient and (b) maximum axial flow rate coefficient.	78
Figure 4.23	Total pressure coefficient versus $4b/D_1$ for constant axial flow coefficient ($\varphi_a = 0.25$) or constant radial flow coefficient ($\varphi_r = 0.43$).	79
Figure 4.24	A double-outlet squirrel-cage fan.	79
Figure 4.25	Total pressure variation in channel 1 versus volumetric flow rate in both channels (C1 and C2 denotes channels 1 and 2, respectively). The volumetric flow rate and total pressure are measured in m^3/s and millimetre of water, respectively.	80
Figure 4.26	Total pressure variation in channel 2 versus flow rate in both channels. The volumetric flow rate and total pressure are measured in m^3/s and millimetre of water, respectively.	80
Figure 4.27	Variation of double-outlet fan efficiency versus flow rate in both channels. The volumetric flow rate is measured in m^3/s .	81
Figure 4.28	A comparison between the double-outlet fan (at three different operating conditions) and a similar industrial single-outlet fan. The gage static pressures are measured in millimetre of water.	81
Figure 5.1	A frequency spectrum of the sound of a squirrel-cage fan.	87
Figure 5.2	An unbounded region with a moving solid body.	89
Figure 5.3	Boundary of a centrifugal fan for implementation of the thin-body boundary element method.	91
Figure 5.4	Comparison between head coefficient (a) and sound-power level (b) of the fans with inward inlets of different diameters and a fan with no inlet nozzle.	94
Figure 5.5	Head coefficient (a) and sound-power level (b) of the fans with different rotor-inlet annular clearance.	95
Figure 5.6	Spectrum of pressure fluctuation on a point close to the cut-off (a) and another point at $\theta = 240^\circ$ (b) along the volute mid-plane. The blade passing frequency (BPF) is shown in the dashed line.	96